Technical Report No. 1
Contract N6 ori 071 (54)

CRYSTAL PERFECTION IN ALUMINUM SINGLE CRYSTALS

T. S. Noggle and J. S. Koehler
Department of Physics
University of Illinois
Urbana, Illinois

September, 1954

U. S. Navy Department
Office of Naval Research
Washington, D. C.

ABSTRACT

A high resolution x-ray diffraction technique has been employed on annealed single crystals of aluminum in order to arrive at an estimate of dislocation densities and distributions. This work indicates that in annealed aluminum crystals the majority of the dislocations are present in an essentially random array with densities of the order of 10^6 lines/cm^2. Small angle boundaries, which are commonly present, contribute about 10^4 to 10^5 lines/cm^2 to the dislocation density. Comparison of crystals obtained by growth from the melt and by recrystallization indicates that there are no basic differences in the degree of crystal perfection obtained using the two methods of growth.

Crystal Perfection In Aluminum Single Crystals

T. S. Noggle and J. S. Koehler
University of Illinois, Urbana, Illinois

INTRODUCTION

It is generally accepted at the present time that a type of crystal imperfection called a dislocation plays a very important role in determining many of the properties of crystals. The influence of dislocations on the properties of crystals arises as a result of the inherent properties of a dislocation and its interaction with other dislocations or other types of lattice defects. Despite the recognized importance of the role of dislocations on properties such as mechanical strength, damping and electrical resistance, there has been but little work done toward obtaining direct estimates of dislocation distributions and densities. This state of affairs is primarily due to the lack of completely satisfactory methods of measuring dislocation densities and distributions. Recently developed x-ray diffraction techniques[1][2][3] offer hope of improving this situation, and as applied particularly to metal crystals, are capable of giving semi-quantitative estimates of dislocation densities. In addition these methods can detect the presence of and measure the magnitude of a particular type of dislocation distribution commonly referred to as a small angle boundary. Information of this kind is of importance in the interpretation of physical behavior in terms of dislocation theory.

The present investigation was carried out to assess the possibilities of using x-ray measurements to determine the dislocation structure of reasonably well annealed aluminum single crystals. In addition, single crystals of aluminum obtained by different growing methods were examined to ascertain if there were measurable differences in the degree of crystal perfection and if any basic differences in the type or distribution of the imperfections could be detected.

GENERAL CONSIDERATIONS

X-ray diffraction theory predicts that reflection of x-rays from a set of lattice planes in a perfect crystal should occur over an angular range of a few seconds of arc. In practice, it is found that most crystals give reflections over an angular range in excess of one minute. This spread in the angular range can be interpreted in terms of a mosaic block structure in which the angular range of orientations is given by the spread of the reflection. This concept of a mosaic structure was initially introduced by Darwin[4] to account for the observed intensities of reflections from real crystals. Theory indicated that the observed intensities could be accounted for by a mosaic block size of mean diameter 10^{-4} to 10^{-5} cm. This mosaic structure can be interpreted in terms of dislocation distributions in which the boundaries between the blocks are defined by dislocations, and for the block sizes above would give dislocation densities of 10^{8} to 10^{10} lines/cm^{2}.

In addition to the spread in the reflection angle which arises from the tilting of the blocks, contributions to the angular range of the reflections should arise due to the size of the mosaic blocks and from the strains associated with the presence of dislocations.

Cottrell[5] discusses the interpretation of the spread of x-ray reflections in terms of possible dislocation models for the case of tilting of the mosaic blocks. The type of model that he indicates should give the most reliable estimates of dislocation densities consists of a linear array of blocks of mean size l, each block tilted by the angle α relative to its neighbors, α being randomly positive or negative. For this case, the probable angular deviation ε between two points in the crystal separated by the distance L is given by:

$$\varepsilon = \alpha\sqrt{\frac{L}{l}} \qquad (1)$$

Assuming that the angle α is due to a single dislocation in the block boundary, the probable angular deviation is related to the dislocation density by the relation:

$$\varepsilon = b\rho^{3/4}\sqrt{L} \qquad (2)$$

where b is the Buerger's vector of a dislocation and ρ is the dislocation density in lines/cm^2.

Extension of this theory to the two-dimensional case and to a derivation of the distribution function of the one-dimensional model leads to results similar to equation (2) in that the mean

square deviation increases with increasing sample size. The conclusion from this is that if dislocation distributions are essentially random, then the expected angular deviations will increase with increases in the crystal size or of the region investigated. This point can be checked experimentally. In addition, the tilting block model indicates that this source of angular spread of the reflections is independent of the reflection angle and offers the possibility of sorting out its contributions from other sources of line broadening which are dependent on the diffraction angle.

The particle size broadening equation gives the increase in the angular spread of the reflection associated with the size of the coherently reflecting region.(6) This relation is:

$$w - w_0 = \frac{0.9\lambda}{l \cos \theta} \qquad (3)$$

w = experimental line width

w_0 = instrumental line width

λ = wave length of x-rays reflected by the crystal

θ = Bragg angle

l = mean particle size

This equation predicts an increase in the line width due to decrease in the particle size. For a given system (λ, l constant) the line width observed will vary as a function of secant θ. In practice, the application of this relationship to the interpretation of experimental data requires accurate knowledge of the instrumental line widths--particularly in the case of annealed crystals where l

is relatively large and the expected changes in line width are small.

The influence of lattice strains on the angular range of the reflections arises due to the change in the diffraction angle with changes in the interplanar spacing. The shift in the reflection angle is given by:

$$\Delta\theta = - \varepsilon \tan \theta \qquad (4)$$

where ε = strain, θ = diffraction angle.

A uniform strain will simply produce a shift in the diffraction angle without any change in the angular range of the reflection. However, a non-uniform strain will give a contribution to the line width due to variation in ε. The line width increase Δw due to a range of strain $\Delta\varepsilon$ is given by:

$$\Delta w = \Delta\varepsilon \tan \theta \qquad (5)$$

In order to relate equation (5) to dislocation theory, the mean strain due to dislocations in a crystal can be estimated by averaging the strain due to a single dislocation over the region surrounding the dislocation to points midway between adjacent dislocations. This type of calculation can be carried out for edge type dislocations and gives:

$$\sqrt{\bar{\varepsilon}^2} = \frac{b}{R} \sqrt{\log \frac{R}{r_o}} \qquad (6)$$

where: ε^2 = the mean square tensile or compressive strain.

b = the Buerger's vector of a dislocation.

R = the radius of the region occupied by the dislocation

r_o = the radius of a region around the core of the dislocation in which equation (6) is not applicable due to failure of the elasticity equations from which (6) is derived in the region of large strains near the center of the dislocation. This region extends several atomic dimensions around the dislocation and is given a value of 6×10^{-8} cm in subsequent calculations.

Equation (5) gives the mean tensile strain in the region below a positive edge dislocation, or the mean compressive strain in the region above the dislocation. Thus, the range of strain will be twice the mean strain. Taking this into account, and also that $R \simeq \frac{1}{2}$ we get:

$$\Delta w = 4 \rho^{1/2} \sqrt{\log \frac{1}{2r_o \rho^{1/2}}} \cdot \tan \theta \qquad (7)$$

The increase in line width predicted by this equation would be due only to edge type dislocations since screw type dislocations introduce no dilation of the lattice.[4b]

In addition to the sources of line broadening discussed above, small angle boundaries are usually present in metal crystals and are detected readily by high angular resolution x-ray diffraction techniques. They are observed in an x-ray reflection as a displacement between one portion of the reflection and another. The angle associated with this displacement is a direct measure of the angular misorientation occuring at the boundary. The simplest type of boundary that can be constructed using dislocations, consists of a

sheet of parallel edge type dislocations of the same sign with a mean spacing h between the dislocations. For small angular misorientations, the angle of tilt of the boundary is: $\alpha = \frac{b}{h}$ (8)
where: α = tilt angle of boundary b = Buergers vector of the dislocations

High resolution x-ray diffraction methods have been applied to metal single crystals by several investigators, and their results have indicated that a higher degree of crystal perfection than heretofore expected sometimes exists in carefully handled single crystals obtained by recrystallization. Guinier and Tennevin[1] using a focusing Laue method, reported a maximum disorientation in certain aluminum specimens of less than 30 seconds of arc over regions involving about 30 mm^3. In terms of the tilting block model for estimating dislocation densities (equation 2), this gives a dislocation density of $\rho = 2.3 \times 10^5$ lines/cm. Lambot, Wassamillet, and Dejace[2] employing a method similar to that used in the present investigation, reported for Al and Fe single crystals a maximum disorientation of 50 seconds of arc. This corresponds to a dislocation density of about 7.5×10^6 lines/cm^2. Gay, Hirsch and Kelly[3] using a micro beam technique, report the upper limit for the dislocation densities in annealed aluminum as 3×10^8 lines/cm^2. In that their work was carried out on polycrystalline material, it is not clear that their results are comparable to results obtained on single crystals.

EXPERIMENTAL METHODS

High purity aluminum single crystal specimens were prepared in the form of square tensile specimens 1 cm square by 6 cm long in the reduced section of the bars. One group of specimens was prepared by the strain-anneal method of Schwope, Shober, and Jackson[7]. The other group of specimens were prepared by the "soft mold" method[8]. Both groups of specimens were prepared from the same bars of hi-purity aluminum (99.99* % Al)*.

After the appropriate crystal growing cycles had been carried out, the specimens were etched in a macroetch solution[9] which was capable of showing orientation differences of about 1/2°. The presence or absence of visible disorientations on the etched specimens was used as a criterion for sorting them into satisfactory and unsatisfactory categories. Most of the specimens processed by the strain-anneal method required an anneal of 20 - 50 hours at 650°C to eliminate isolated grains that remained after the growing cycle. The yield of satisfactory specimens was about the same for each method, being slightly better than 50 per cent.

X-RAY METHODS

The x-ray method used was essentially the same as that described by Lambot, Vassamillet, and Dejace[2]. Our experimental set-up is indicated schematically in figure 1. It employed a G.E. CA7, copper target, x-ray tube with the beam taken from the line focus port at about 4° to the plane of the target. A bent crystal

*Supplied by Aluminum Research Laboratories, Aluminum Company of America.

monochromator intercepted this beam and reflected a monochromatic beam which was convergent in the horizontal plane and divergent in the vertical plane. When properly adjusted the monochromator gave a fine line focus in which the Cu - Kα doublet was cleanly resolved. The characteristics of the beam obtained from the monochromator are listed in Table 1.

Specimens were held in a goniometer which could be adjusted so that the plane of the surface being investigated coincided with the vertical axis of rotation of the goniometer which in turn had been adjusted to coincide with the monochromator focus. The orienting of specimens to obtain reflections was facilitated by prior knowledge of the orientation obtained by the back reflection method.

In the adjusting of the monochromator, it was found convenient to employ a long focal length microscope to observe the focus on a fluorescent screen. Use of this method improved the speed and reproducibility of adjustment over that of the photographic method. In addition, the use of a portable Geiger counter to detect and locate the reflection from the specimen facilitated the accurate adjustment of the specimen for maximum intensity of reflection.

Reflections were registered on film at a distance of one meter from the specimen. Exposure times varied from 10 minutes for the (111) reflection from aluminum to about 2 hours for the (333) reflection. The films were scanned on a L and N microphotometer and line widths measured at one-half the maximum film

density. Figure 2 shows several reflections obtained by this method. Figure 3 shows a typical microphotometer record obtained from an aluminum specimen.

Aperturing of the incident beam was carried out to test the predictions of the theory based on the tilting block model. This was accomplished by inserting lead slits into the path of the incident beam at a point about 1 mm. in front of the specimen. By this means the vertical height of the beam at the specimen could be varied from 0.1 mm to the full beam height without disturbing the monochromator or specimen adjustments and without sensibly affecting the angular aperture of the incident beam. These aperturing tests were carried out on aluminum specimen D, grown from the melt, which fortuitously combined the attributes of a good degree of crystal perfection and an orientation such that the (111) reflection could be obtained under nearly optimum experimental conditions. In addition, similar tests were carried out on a quartz crystal using the $(2\bar{1}0)$ reflection. This reflection occurs at a Bragg angle very nearly the same as the (111) reflection from aluminum.

In order to determine the angular dependence of the line widths, a number of reflections which covered the range of reflection angles possible were obtained from one face of aluminum specimen D. All reflections were obtained from the same region of the specimen. Three reflections covering about the same angular range were obtained from the quartz crystal for comparison.

A survey was carried out on a number of aluminum specimens

for comparison between the strain-anneal and the melt-grown specimens. Reflections were obtained from each of the four faces of a specimen, usually near the central region along the length of the specimen. Six specimens, three of the strain-anneal and three of the melt-grown, were checked at two different positions separated by about 3 cm along the length of the specimen. No significant differences in the degree of crystal perfection was observed between the top and bottom regions, so the balance of the specimens were examined only near the center.

RESULTS

Aperturing Tests: The results of the aperturing tests on line widths are tabulated in Table 2 and summarized graphically in figure 4. The interpretation of the behavior observed is reasonably direct, but requires some understanding of the geometry of the experiment.

If all possible paths are considered by which a ray can arrive at and be reflected from a point on the specimen which is centrally located with respect to one of the lines in the focus, it is found that there is a vertical angular range (vertical angular aperture) of about $3/4^{\circ}$ over which this can occur. As a result, the reflection from this point is registered on the film as a short arc whose vertical length corresponds to about $3/4^{\circ}$ and whose horizontal width is determined by the material giving the reflection and by the spectral range present in the x-ray beam. Points on the specimen which are close enough to each other will

give reflections which overlap and reinforce the intensity at the film. This condition varies with the vertical position along the focus. For reflection from points above and below the midpoint of the focus, the vertical angular aperture is reduced, and the direction of the ray producing the center of the reflected arc will no longer be horizontal, but will have a small vertical inclination. At the extremities, the vertical aperture is very small and the mean paths are inclined at about 2° to the horizontal. This can be seen in the reflections shown in figure 2 in which the lines taper off in intensity at either end due to the reduction of the vertical aperture at the top and bottom ends of the focus. The central portions of the lines which are uniform in intensity are from the central region of the focus where changes in the vertical aperture and the inclination of the mean path are small. This region of uniform intensity in the reflection is estimated to correspond to the center 4 mm. of the focus, and this is the region in which the slits were used to define the beam height. In this portion of the reflection, the experimental line width is determined by instrumental contributions* and by the angular variations present in the material in an area defined by the focal width and about 1 mm. of length along the focus.

Inserting a slit to define the beam height at the specimen will not affect the line width in the central part of the reflection

* The instrumental contributions to the widths of reflections obtained with our experimental set-up have been treated in some detail by Lambot, Vassamillet, and Dejace.(2) Except for the contribution due to spectral width, the instrumental contributions for the reflections observed in the aperturing tests are quite small and lead to no serious errors if neglected.

until the slit height becomes less than the maximum separation distance of points giving overlapping reflections. For slits less than this critical size, the area contributing to the reflection is reduced. In the aperturing experiments, this critical size corresponds to about 1 mm., and for slits in the range of 0.5 to 1.0 mm the variation in the line widths qualitatively follows the behavior predicted by equation (2). Below 0.5 mm, the gradual upturn and sharp increase in the line width is believed due to scattering of the incident beam at the edges of the slit. This factor would become relatively more pronounced with decreasing slit heights as is evident in the large values of the line widths for the 0.1 mm slit.

Due to the limited range of slit sizes for which the line widths vary, it is not possible to check in detail whether these changes follow the square root relation of equation (2). A rough check can be made from the ratio of the line widths for the 1.0 mm and 0.5 mm slit sizes. This ratio is 1.46 for the aluminum specimen and 1.40 for the quartz. The ratio expected from equation (3) is 1.41. The agreement between experiment and the tilting block model theory is surprisingly good, particularly in view of serious doubts that arise as to the applicability of a theory based on a one-dimensional model to a three-dimensional (or at best quasi two-dimensional) system. The important result of these measurements is that the behavior observed is qualitatively consistent with the behavior expected from a system containing a random dislocation distribution.

Further consideration of the applicability of equation (2) to observations made during this investigation reveal some features which are of interest. If we use equation (2) to calculate probable angular deviations for widely separated points in the crystal (L = 1 cm) for dislocation densities in the range of 10^6 lines/cm^2 to 10^8 lines/cm^2, we obtain the following values for the probable angular deviation:

$$\varphi_{\rho=10^6} \simeq 2.2' \qquad \varphi_{\rho=10^7} \simeq 13' \qquad \varphi_{\rho=10^8} \simeq 1^\circ 9'$$

When the full beam is employed, the reflection obtained comes from a region on the specimen along a line about 1 cm in length. We can readily detect horizontal deviations in the position of the reflection of about 1 min. and vertical deviations of about 10 min. In the absence of small angle boundaries, no horizontal deviations from the mean reflection position were observed that amounted to more than 1 or 2 minutes. No vertical deviations were detected. This indicates that either the dislocation densities of the specimens observed were of the order of 10^6 lines/cm^2 or less, or that the tilting block model from which equation (2) is derived is not a good representation of the situation in a real crystal.

Variation of Line Width with Diffraction Angle: The results of the measurements made to determine the dependence of the line width on the diffraction angle are tabulated in Table 3 and summarized graphically in figures 4 and 5. It is not possible to decide from these graphs whether the data follows the tangent θ relation for strain broadening, or the secant θ relation for particle size broadening. The results obtained on the quarts are

somewhat indefinite due to scatter in the points obtained. Dislocation densities calculated from the slopes of the curves in figures 4 and 5 are tabulated in Table 4 along with the values calculated from equation (2). The agreement between the dislocation densities estimated in the aluminum specimen by the tilting block model and the particle size relation is quite good.

The low dislocation densities obtained from the strain broadening relation as compared with the densities estimated from the tilting block model and from the particle size relation indicates that strains of the type considered in the derivation of equation (6) are quite small. The dislocation densities tabulated in Table 4 for particle size broadening are calculated under the assumption that strain broadening is negligible, and the strain broadening values assume that particle size broadening is negligible. If the value for dislocation densities given by the tilting block model and by the particle size broadening relation are accepted as the most reliable estimates of the dislocation density in the aluminum crystal examined, the low dislocation density obtained using the strain broadening relation can only be consistent with tilting block and particle size densities if the dilations present are much smaller than one would expect from most dislocation arrangements. It can be consistent if:

1. Screw type dislocations predominate in annealed crystals. This appears to be a reasonable possibility, since the strain energy of an edge type dislocation is about 50 per cent greater than that of a screw dislocation.

2. Edge type dislocations, when present in annealed crystals are in arrays which minimize the strain energy of the crystal. One dislocation array which is commonly observed in metal crystals is the small angle boundary.

Survey of Aluminum Single Crystals: Comparison of the strain-anneal specimens (numbered series) with the melt-grown specimens (alphabet series) from the survey results as tabulated in Table 5 indicates that on the average the former show a slightly better degree of crystal perfection. The rather surprising aspect of this survey is that there were a number of melt-grown specimens which were comparable in all respects to the strain-anneal specimens. In general, the degree of crystal perfection present in the melt-grown specimens is much better than would be expected from information available in the literature.

In the melt-grown specimens, the number of small angle boundaries intercepted by the beam was determined in part by the angle the line of the focus made with the specimen axis. When the focus was perpendicular to the specimen axis, it intercepted on an average three times as many boundaries as when it was parallel to the specimen axis. This indicates that the boundaries tend to run parallel to the specimen axis (and the growth direction). No indications of a preferred direction of the boundaries was observed in the strain-anneal specimens.

The density of dislocations in the small angle boundaries is comparatively small. For the strain-anneal specimens, the

average density of dislocations in boundaries is 6.2×10^4 lines/cm^2, and for the melt-grown specimens 1.4×10^5 lines/cm^2. The line widths of the strain-anneal specimens tend to be slightly smaller than those of the melt-grown specimens. Annealing of several melt-grown specimens produced no detectable changes in the line widths. The average corrected line widths for both groups of specimens are 0.62' for the melt specimens and 0.45' for the strain-anneal specimens. The latter value is about the same as observed for the $(2\bar{1}0)$ reflection from the quartz. The dislocation densities corresponding to these line widths are 6×10^6 lines/cm^2 for the melt specimens and 3.5×10^5 lines/cm^2 for the strain anneal specimens.

Some insight as to one of the sources of variation in line widths from specimen to specimen is given by a series of microphotometer measurements of the (111) reflection from specimen D and the $(2\bar{1}0)$ reflection of the quartz. Each reflection was scanned at 0.5 cm intervals along its length over the central 5 cm of the line where the film density in the reflection was uniform. The root mean square deviation of the measurements from the aluminum specimen amounted to 20 per cent of the corrected line width, while the deviation for the quartz was 2 per cent. Close visual examination of the aluminum lines indicated that small bulges were present on the lines (compare a and b in figure 2). Some, but not all of the melt-grown specimens gave reflections with this type of variation in the lines, whereas the strain-anneal specimens rarely showed this type of variation. These variations

are thought to correspond to small angle boundaries which are not resolved and represent angular disorientations of less than about 20" of arc.

The comparable degree of perfection observed in the quartz and aluminum specimens is consistent with previous work which employed this x-ray method.[2] Comparison of our results, which were obtained by reflection, with previous results obtained in transmission[2] do not indicate any sensible differences in the degree of crystal perfection observed. This point is of some importance, since the reflection method "sees" only a thin layer at the surface and the question naturally arises as to whether these surface observations are also applicable to the interior of the crystal. In that the transmission measurements mentioned above were made on 0.5 mm thick specimens, it appears that our measurements in reflection are representative of the material to a depth comparable to this.

The unexpected high degree of crystal perfection in the melt-grown specimens is probably associated with the crystal growing method employed. No attempt has been made to date to ascertain which of several possible factors are of importance. The factors that are different in the "soft-mold" method from more conventional methods are the strength (or softness) and the radial thermal insulation provided by the mold material. The softness of the mold material reduces the possibility of strain due to differential thermal contraction in specimens "keyed" in the mold, and in addition, permits easy removal without the danger of accidentally

damaging a specimen. The radial thermal insulation provided by the mold material combined with extraction of heat by conduction from the bottom of the mold favors a truly axial heat flow in the specimen during solidification. This last factor is thought to be the more important of those discussed.

CONCLUSIONS

The use of high resolution x-ray diffraction methods on annealed crystals offers good possibilities of obtaining considerable information about the dislocation densities and distributions. The present work indicates that in annealed aluminum single crystals, the majority of the dislocations are present in essentially random arrays and in densities of about 10^6 lines/cm^2. Small angle boundaries contribute but little to the overall dislocation density, contributing on the average about 10^4 to 10^5 lines/cm^2.

No basic differences were observed between aluminum single crystals prepared by the strain anneal method and those grown from the melt. The major difference between the two types of crystals is that <u>on the average</u> the number and angular range of small angle boundaries is less in the strain anneal crystals.

Additional work is needed to confirm and expand the results of this investigation. Extension of the work on the statistics of dislocation distributions--both experimental and theoretical--is particularly desirable. Experimental techniques different from those employed in this work should be investigated.

ACKNOWLEDGEMENT

The authors are grateful to Professor A. Guinier for help with this method during his period of residence as Visiting Professor of Metallurgy in the Department of Mining and Metallurgy at the University of Illinois.

REFERENCES

1. Guinier, A. and Tennevin, J. Acta Crystallographica, 2, p. 133, 1949.

2. Lambot, H., Vassamillet, L., and Dejace, J., Acta Metallurgica, 1, p. 711, 1953.

3. Gay, P., Hirsch, P.B., and Kelly, A., Acta Metallurgica, 1, p. 315, 1953.

4. Darwin, C. G., Philosophical Magazine, 27, pp. 315 and 675, 1914.

5. Cottrell, A. H., Dislocations and Plastic Flow in Crystals (a) 100, (b) 40 Oxford University Press, London, 1953.

6. Guinier, A., Imperfections in Nearly Perfect Crystals p. 402, John Wiley and Sons, 1952.

7. Schwope, A. D., Shober, F. R., and Jackson, L. R., Creep In Metals. NACA TN 2618, 1952.

8. Noggle, T. S., Rev. Sci. Inst. 24 p. 184, 1953.

9. Beck, P.A., Kremer, J.C., Demer, L.J., and Holzworth, M.L., Trans. AIME 175 p. 372, 1948.

TABLE I

Separation of $K\alpha_1$ and $K\alpha_2$	.085 mm
Width of $K\alpha_1$ at one-half maximum intensity	.068 mm
Width of $K\alpha_2$ at one-half maximum intensity	.058 mm
Full width at background intensity level	.20 mm
Vertical height	10 mm
Horisontal angular aperture . . . approximately	1°
Vertical angular aperture . . . approximately	3/4°

TABLE II

		Line Widths in Minutes				
		α_1		α_2		
Specimen	Aperture Slit Height mm	Experimental Width*	Corrected For Spectral Width	Experimental Width*	Corrected For Spectral Width	Average Corrected Width
Aluminum	0.1	1.72	1.27	1.42	.82	1.04
D	0.2	1.10	.65	1.08	.48	.56
	0.5	1.07	.62	1.01	.41	.52
(111)	1.0	1.23	.78	1.33	.73	.76
Reflection	2.0	1.08	.63	1.05	.45	.54
	5.0	1.29	.84	1.23	.63	.74
Quartz	0.1	1.28	.83	1.15	.55	.69
$(2\bar{1}0)$	0.2	.95	.50	.93	.33	.42
	0.5	.93	.48	.95	.35	.42
Reflection	1.0	1.08	.63	1.15	.55	.59
	2.0	1.07	.62	1.23	.63	.62
	5.0	1.09	.64	1.21	.61	.62

* Average of three microphotometer scannings on the lines.

TABLE XII

Specimen and Reflection	Average Line Widths in Minutes				
	Experimental Width		Corrected* Width		Average Corrected Width
	α_1	α_2	α_1	α_2	
Aluminum Specimen D					
(111)	1.32	1.38	.83	.74	.78
(220)	2.09	1.65	1.21	.49	.84
(222)	2.15	2.26	.93	.66	.79
(331)	2.88	3.12	.86	.45	.66
(422)	4.82	5.44	1.26	.70	.98
(333)	11.16	14.30	2.16	1.04	1.60
Quarts					
(2$\bar{1}$0)	1.08	1.09	.59	.45	.52
(4$\bar{1}$0)	1.50	1.80	.29	.20	.24
(5$\bar{2}$4)	7.36	8.52	1.16	.04	.60

* Corrected for spectral width and vertical aperture. See Reference 2.

TABLE IV

Specimen	Dislocation Densities			
	Tilting Block		Particle size	Strain
	I	II		
Aluminum D	6.2×10^6	1.18×10^6	8.6×10^6	1.5×10^4
Quarts	3.8×10^6	6.9×10^5	2×10^5--5×10^6	4×10^2--1×10^4

I -- $L = 7.6 \times 10^{-3}$ cm = average width at the specimen

II -- $L = 1 \times 10^{-1}$ cm = effective vertical beam height at the specimen

TABLE V

Specimen	Reflection	Mean Line Widths Uncorrected α_1	Mean Line Widths Uncorrected α_2	Mean Line Widths Corrected for Spectral Width α_1	Mean Line Widths Corrected for Spectral Width α_2	Avg. no. of Small angle Boundaries*	Average Boundary Angle	Maximum Disorientation
7	220	1.45	1.52	.63	.42	1.8	1.1'	3.0'
10	220	1.42	1.36	.60	.26	5.0	1.2'	5.2'
	311	1.34	1.55	.29	.15			
13	220	1.39	1.43	.57	.33	2.8	0.9'	3.4'
14	311	1.51	1.74	.46	.34	2.3	1.2'	2.4'
15	220	2.12	1.83	1.30	.73	1.3	0.9'	1.4'
18	200	1.04	0.90	.51	.19	1.0	0.7'	1.5'
	311	1.29	1.49	.24	.09			
22	311	1.62	1.81	.57	.41	0	---	---
D	111	1.32	1.38	.87	.78			
	220	2.09	1.65	1.27	.55	.7	.8'	1.5'
	311	1.87	2.14	.82	.74			
E	220	1.60	1.73	.78	.63	1.4	.8'	.8'
F Annealed	220	1.30	1.45	.48	.35	1.7	4.8'	34.4'
	311	1.58	1.83	.53	.43			
H	311	2.32	2.46	1.27	1.06	.8	2.5'	5.5'
L	311	1.50	1.62	.45	.22	1.0	2.25'	4.1'
M	200	1.77	1.64	1.24	.93	.3	.7'	.7'
	311	1.33	1.58	.28	.18			
N	311	1.61	1.87	.56	.47	6.2	3.4'	13.5'
P	220	1.67	1.68	.85	.28	1.5	1.4	2.61'
	311	1.91	1.93	.86	.53			
Q	311	1.99	2.02	.94	.62	3.0	1.72'	5.16'
S	220	1.63	1.65	.81	.55	4.5	1.7'	14.4'
T	200	1.12	1.10	.59	.39	1.4	2.8'	7.4'
	220	1.22	1.36	.40	.20			
V	220	2.18	2.10	1.13	1.00	2.2	1.8'	7.4'
	311	1.63	1.55	.58	.15			
PCI	220	1.75	1.66	.93	.56	2.0	1.6'	5.2'
	311	2.10	2.16	1.05	.76			

* These values are obtained by counting the discontinuities on each of the films obtained from a given specimen and dividing this count by the number of films. This gives approximately the average number of small angle boundaries that would be intersected by a line on a crystal 1 cm in length.

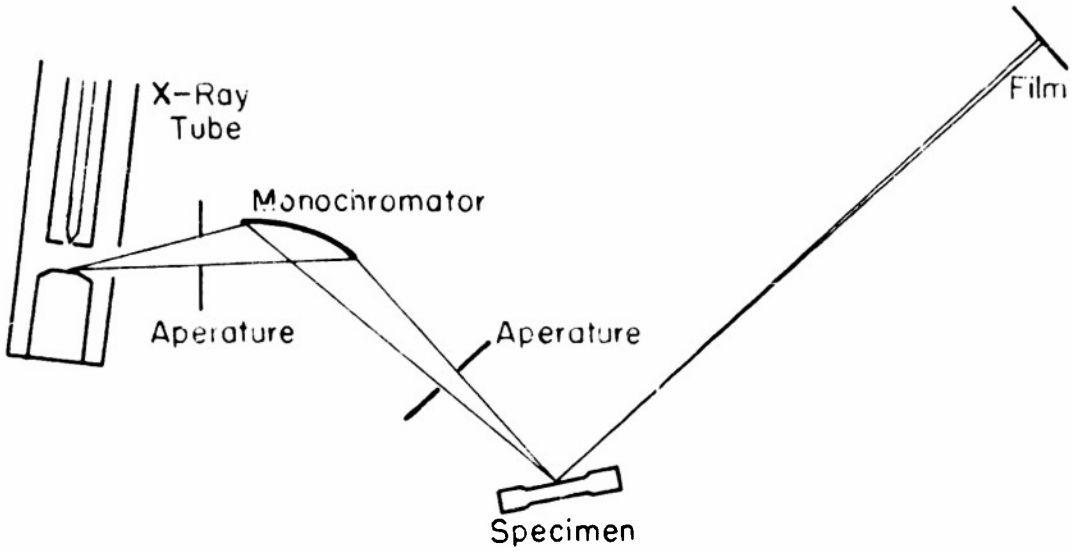

Fig. 1
Schematic Diagram of Experimental Set-up

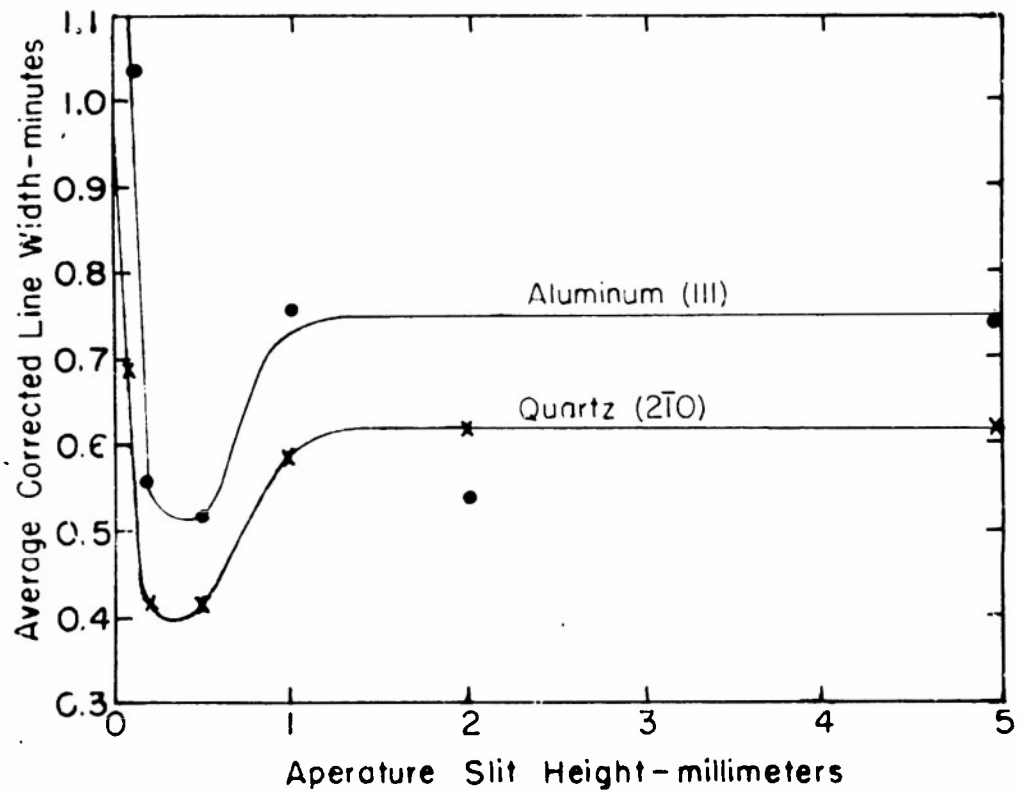

Fig. 4

Effect of Aperoturing on the line widths of the (111) reflection from Aluminum and the (2$\bar{1}$0) reflection from Quartz.
Cu. $K\alpha$ Radiation

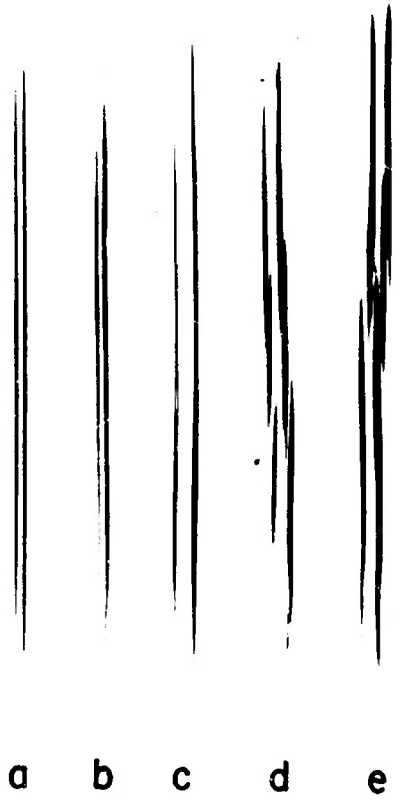

Figure 2. a. Quartz (2TO); b. Al. specimen D(111); c. Al. specimen 18 (311); d. Al. specimen 10(220); e. Al. specimen 5 (220). (Numbered specimens obtained by strain anneal, lettered specimens from the melt).

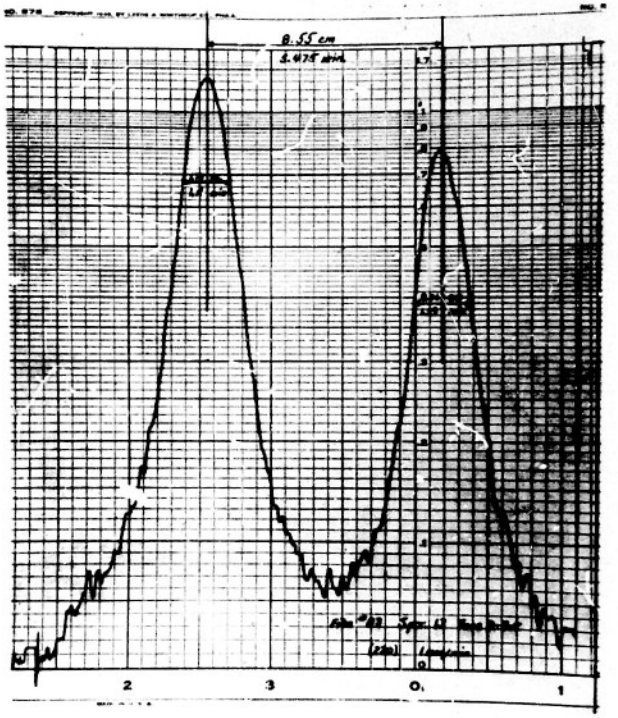

Figure 3. Typical Microphotometer record obtained from films.

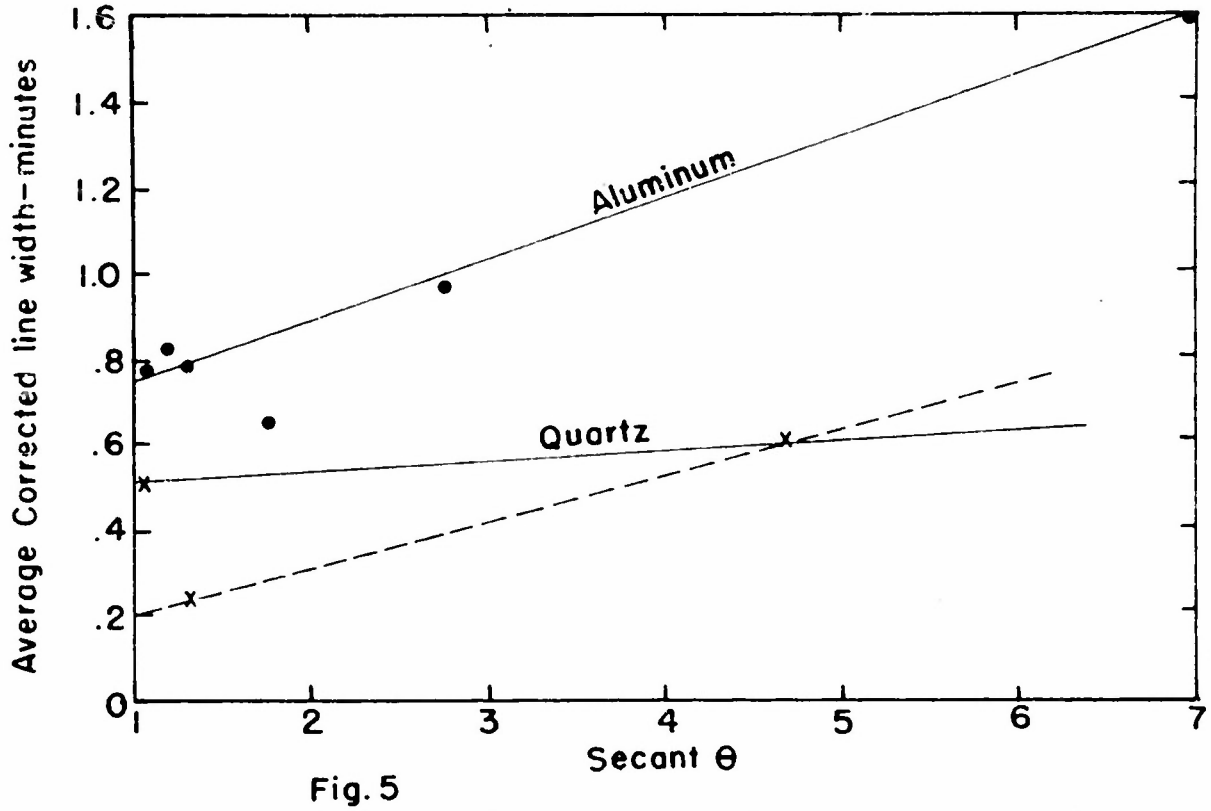

Fig. 5
Variations in line widths as a function of Secant θ

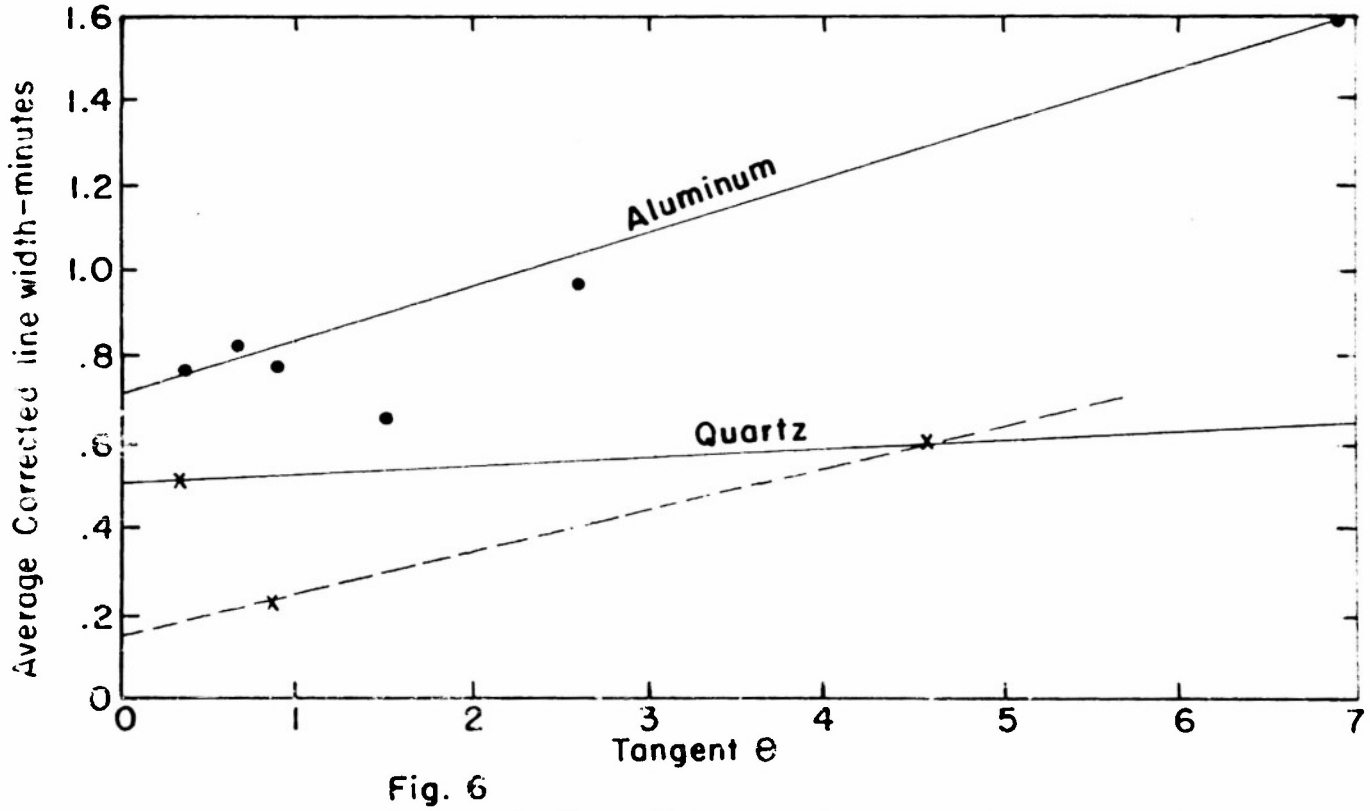

Fig. 6
Variations in line widths as a function of Tangent θ

DISTRIBUTION LIST

for

N6 ori 071 (54)

A. Government Distribution

1. Department of Defense

Research and Development Board
Information Office Library Branch
Pentagon Bldg.
Washington 25, D. C. (2 copies)

Armed Services Technical Information Agency
U. B. Bldg.
Dayton 2, Ohio (5 copies)

2. Department of the Navy

Chief, Bureau of Aeronautics
TD-4
Navy Department
Washington 25, D. C.

Chief, Bureau of Ordnance
Rea
Navy Department
Washington 25, D. C.

Chief, Bureau of Ships
Code 300
Navy Department
Washington 25, D. C.

Chief of Naval Research
Office of Naval Research
Washington 25, D. C.
Attn: Physics Branch (Code 421) (3 copies)

Director
Naval Research Laboratory
Technical Information Officer (Code 2000) (9 copies)
Code 2021 (2 copies)
Washington 20, D. C.

Director
Office of Naval Research Branch Office
150 Causeway Street
Boston 14, Massachusetts

Director
Office of Naval Research Branch Office
346 Broadway
New York 13, New York

Director
Office of Naval Research Branch Office
86 East Randolph Street
Chicago 13, Illinois

Director
Office of Naval Research Branch Office
100 Geary Street
San Francisco 9, California

Director
Office of Naval Research Branch Office
1031 East Green Street
Pasadena 1, California

Officer in Charge
Office of Naval Research London Branch Office
Navy No. 100
Fleet Post Office
New York, New York (2 copies)

Physics Department
Post Graduate School
U. S. Naval Academy
Annapolis, Maryland

Librarian
U. S. Naval Post Graduate School
Monterey, California

U. S. Naval Electronics Laboratory Library
San Diego 52, California

Director
Physics Research
Naval Ordnance Laboratory
White Oaks, Maryland

Director
Physics Research
Naval Ordnance Test Station
Inyokern
China Lake, California

3. Department of the Air Force

Commanding General
Air Research and Development Command
Attn: Office of Scientific Research
Post Office Box 1395
Baltimore 3, Maryland (2 copies)

Air Adjutant General
Mail and Receiving Management Division
Headquarters, U.S.A.F.
Washington 25, D. C.

4. Department of the Army

Commanding Officer
Engineering Research and Development Laboratories
Fort Belvoir, Virginia
Attn: Technical Intelligence Branch

Office of Ordnance Research
Box CM, Duke Station
Durham, North Carolina (2 copies)

Signal Corps Engineering Laboratory
Fort Monmouth, New Jersey
Attn: Technical Information Officer

5. Department of Commerce

Office of Technical Services
Technical Reports Section
Department of Commerce
Washington 25, D. C. (2 copies)

Director
National Bureau of Standards
Washington 25, D. C. (2 copies)

Director
National Bureau of Standards
Corona, California

6. Other Agencies

National Research Council
Division of Physical Sciences
National Academy of Sciences
Washington, D. C.

Director
National Science Foundation
Washington 25, D. C.

U. S. Atomic Energy Commission
Technical Information Service
P. O. Box 62
Oak Ridge, Tennessee